Strain Engineering of the Magnetocaloric Effect in MnAs Epilayers

D. H. Mosca,[1] F. Vidal,[2] and V. H. Etgens[3]

[1]*Departamento de Física, UFPR, Centro Politécnico C. P. 19091, 81531-990 Curitiba PR, Brazil*
[2]*UPMC-Université Paris 6, UMR 7588, INSP, 140 rue de Lourmel, Paris, F-75015 France*
[3]*CNRS, UMR 7588, INSP, 140 rue de Lourmel, Paris, F-75015 France*

(Received 13 June 2008; published 19 September 2008)

By using heteroepitaxy on two different GaAs templates, we have investigated the impact of anisotropic strain on the magnetocaloric effect (MCE) of MnAs. The temperature range, spread around room temperature, and the maximal MCE position are markedly different in the two epitaxial systems. Simulated MCE curves, obtained from a model based on the mean-field approximation, are in good agreement with the experimental data, indicating that the entropy variation is magnetic in origin. These results illustrate how strain can be used to tune the MCE in materials with coupled structural and magnetic phase transition and suggest that the MCE of MnAs may find applications in microelectronic circuitry.

DOI: 10.1103/PhysRevLett.101.125503 PACS numbers: 61.50.Ks, 68.60.−p, 75.30.Sg

The magnetocaloric effect (MCE) is an isothermal magnetic-entropy change or an adiabatic temperature change of a magnetic material upon application of a magnetic field. A magnetic refrigeration process based on the MCE represents a promising alternative to conventional gas compression techniques because it is environmentally friendly and quite efficient [1]. Materials exhibiting the conventional MCE present a second-order magnetic transition with the contribution to the entropy change being only of magnetic origin. A first-order magnetic transition induces an enhanced MCE with entropy change that can include a considerable contribution from the lattice through the latent heat [1,2]. Commonly, a first-order transition concentrates the MCE in a narrow temperature range, whereas a second-order transition usually spreads it over a broad temperature range [3].

MnAs compounds display one of the highest MCE neighboring room temperature: the isothermal magnetic-entropy change reaches up to 120 J/kg K for a magnetic field variation of 5 T [2]. The entropic magnetic limit for MCE in MnAs is given by $\Delta S_m = R \ln(2J + 1) = 103$ J/kg K, where R is the gas constant and J the total angular momentum of the magnetic ion [4], assuming magnetic field independence of the lattice and electronic entropy contributions. The MCE of MnAs increases under hydrostatic pressure [4] and reaches up to 267 J/kg K for 2.23 kbar. A so-called colossal MCE has also been obtained when Mn is replaced by a few percents of Fe or Cu, which apparently emulates the effect of an external pressure without significant changes in the density of electronic states at the Fermi level of the alloy [5,6]. These huge entropy changes, with respect to those reported in the pioneering work of Wada *et al.* [7], are believed to come from the lattice through the strong magneto-elastic interaction present in MnAs [2]. However, recent investigation suggests that further study is required to confirm this colossal MCE [8,9].

In MnAs-based materials the MCE is associated with a complex magneto-structural phase transition. α-MnAs crystallizes in a ferromagnetic hexagonal NiAs structure [Fig. 1(a)] stable up to 318 K, when it transforms into orthorhombic β-MnAs [Fig. 1(c)] by a first-order phase transition [10–12]. The ferromagnetic order breaks down in a discontinuous manner by a second-order magnetic phase transition with ferromagnetic interactions between d electrons being progressively weakened by the structural phase transition from α to β, which reduces the Mn-Mn separation and strengthens the Mn-Mn bonding in the hexagonal basal plane. In the β phase, Mn-Mn bonds are stronger in the basal plane and weaker between these planes [13].

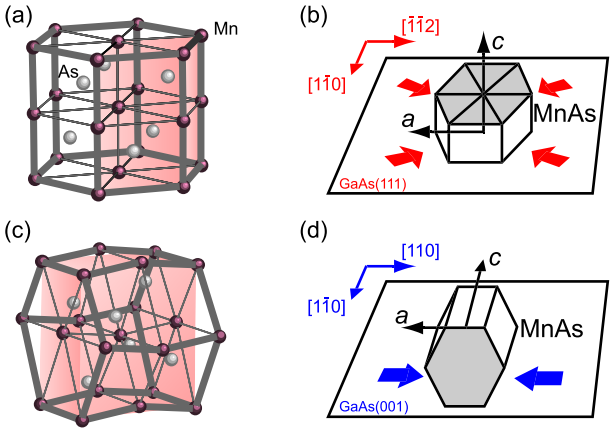

FIG. 1 (color online). (a) NiAs-type crystal structure of α-MnAs consisting of hexagonal planes of Mn and As. (b) Epitaxial scheme of MnAs on GaAs(111) with a biaxial compressive strain indicated by arrows. (c) Crystalline structure of MnAs with an orthorhombically distorted unit cell. (d) Epitaxial scheme of MnAs on GaAs(001) with anisotropic compressive strain indicated by arrows. Unit cell and basal planes of crystal structures are highlighted.

Considering the pressure effect related to the MCE for bulk MnAs compounds and the ferromagnetic interactions in MnAs that are strongly anisotropic and dependent on subtle structural changes, it is possible to anticipate that anisotropic strains like those induced by epitaxy should influence significantly the MCE behavior of MnAs. The aim of the present Letter is to show that MCE related with magneto-structural transition can indeed be tuned by anisotropic strain. This parameter is adjusted by using different epitaxial constraints.

MnAs single-crystal epilayers were grown on GaAs (001) and GaAs(111)B substrates (Si-doped 10^{18} cm^{-3}) by molecular beam epitaxy. Substrates were deoxidized under As flux and a GaAs buffer layer was grown subsequently at 580 °C under As-rich conditions in order to achieve optimal surface quality, as witnessed by reflection high-energy electron diffraction (RHEED) diagrams. 70-nm MnAs epilayers were then grown at 260 °C on these GaAs surfaces with surface reconstructions of (2×2) for GaAs(111)B and $c(4 \times 4)$ for GaAs(001). The epitaxial relations, illustrated in Fig. 1, were checked by RHEED and x-ray diffraction. MnAs samples display a single domain epitaxy with hexagonal c axis along the growth direction for the GaAs(111) template while the hexagonal c axis is along the $[1\bar{1}0]$ direction for the GaAs(001) template. Samples with size of 36 and 56 mm^2 without a protective capping layer were removed from ultrahigh vacuum conditions immediately prior to each magnetic measurement. The MnAs film mass was obtained after thickness determination by cross-sectional transmission electron microscopy and x-ray reflectivity, assuming a density of 6.3 $g\,cm^{-3}$ for MnAs. Magnetic measurements were performed in a superconducting quantum interference device magnetometer (MPMS 2S Quantum Design). The MCE was measured as follows. Temperature dependence of magnetization at different fields (up to 5 T) was monitored with both field and temperature decreasing. Field steps of 0.2 T and sweep rates of 2 K/min were adopted. In-plane magnetic fields were applied parallel to the easy axis with field switching on at 400 K. Although direct determination of the isothermal magnetic-entropy change (ΔS_m) in an adiabatic temperature variation in the presence of a magnetic field is not possible, an indirect verification of the entropy change with temperature (T) and magnetic field (H) can be obtained from magnetization (M) measurements using Maxwell thermodynamic relation $(\partial S/\partial H)_T = (\partial M/\partial T)_H$. Considering that each specific point (T, H) represents an isentropic process, the temperature dependence of ΔS_m can be derived as $\Delta S_m(T, \Delta H) = \int_{H_i}^{H_f} (\partial M/\partial T)_H dH$, where H_i and H_f are the initial and final values of the applied magnetic field, with $\Delta H = H_f - H_i$. This equation predicts a significant MCE when the magnetization variation with temperature is maximum, which occurs at the magneto-structural transition temperature of MnAs.

It has been already shown that the α-β phase transition in MnAs epilayers is strongly perturbed due to the thermal strain incorporated in the epilayer during the cooling step following growth (due to the large lattice mismatch of the MnAs/GaAs system, the misfit strain is already relaxed in the early growth stage). Considering MnAs/GaAs(111), at $T = 275$ K the compressive strain in the basal plane η amounts to 0.82% and leads to the premature appearance of the β phase [14]. Deformation along the c axis has a much lower impact on the phase transition [15], so that it is possible to discuss the magneto-structural behavior using only the strain in the basal plane as a relevant parameter. The phase coexistence allows the compressed α phase to partially relax, thus extending its stability temperature range up to 350 K in the process [14].

We address first the magnetization measurements before discussing the MCE results. A bulklike magnetization behavior at low temperatures for MnAs/GaAs(001) and MnAs/GaAs(111) is observed in Figs. 2(a) and 2(b), respectively. The magnetization thermal evolution reveals an extended α-β phase coexistence with the stabilization of the ferromagnetic α phase at a higher temperature than in bulk MnAs. The structural phase transition itself apparently remains first order at low magnetic fields, as indicated by a little hysteresis (<6 K) separating the magnetization versus temperature branches on cooling and warming procedures. For MnAs/GaAs(111) [Fig. 2(b)], the persistence of the ferromagnetic α phase up to 350 K is explained by the in-plane biaxial strain imposed by the substrate, as already mentioned. For MnAs/GaAs(001), the α-β phase coexistence and stabilization of the ferromagnetic quasihexagonal MnAs at a higher temperature are less pronounced [Fig. 2(a)]. In this case, the crystallographic a

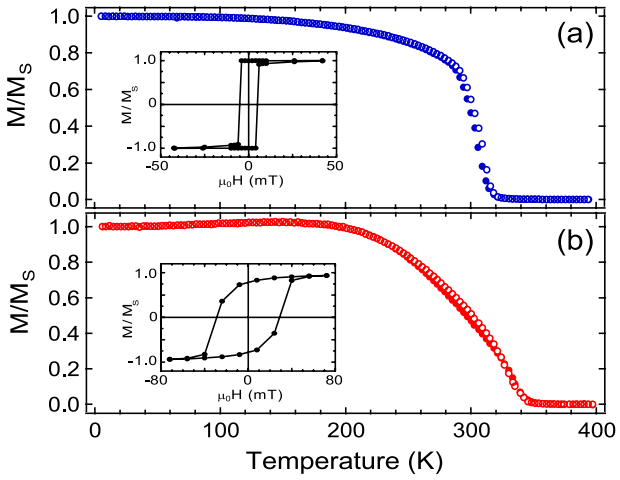

FIG. 2 (color online). Warming (∘) and cooling (●) branches of magnetization measured as a function of temperature in a field of 10 mT applied parallel to the easy magnetic axes for (a) MnAs/GaAs(001) and (b) MnAs/GaAs(111) epilayers. In the inset are shown the inner part of the hysteresis loops measured at room temperature. The coercive fields are 180 and 290 Oe for MnAs epilayers on GaAs(001) and GaAs(111), respectively. Saturation magnetizations are close to 900 G at low temperatures for both MnAs epilayers.

and c axes of MnAs are constrained by the GaAs substrate [16,17]. Magnetocrystalline anisotropy is quite strong in the sample plane, with easy and hard axis being the a and c axis, respectively. Almost square hysteresis loops are observed at room temperature when small magnetic fields H are applied parallel to the easy axis in the film plane, as shown in the inset of Fig. 2.

Figure 3 shows the MCE as a function of temperature and magnetic field intervals for both MnAs epilayers. We observe that MCE curves are rather different for MnAs/GaAs(001) and MnAs/GaAs(111). The shape of the MCE curve does not change significantly as the applied field increases, except for a strong increase of the peaks. This behavior partly reflects the fact that the Zeeman energy overcomes typical elastic energy only above 5 T [18]. Compared to bulk, MnAs epilayers exhibit a MCE spread over a wide temperature range, meaning that for a large temperature difference between a hot and a cold reservoir it is possible to extract a significant amount of heat. As shown in Fig. 3, smaller magneto-structural transition temperature intervals correspond to larger values of maximal ΔS_m. The area below MCE curves defines the refrigerating power of the material. For bulk MnAs, this value obeys an upper limit given by $-M_S \Delta H$, with ΔH being the field variation and M_S the saturation magnetization. The α-MnAs fraction sensitivity to epitaxial constraints leads to significant changes in the M_S values around room temperature, which could explain that the refrigerating power is not constant for different MnAs samples. We observe that a maximum refrigerating power of 774 J/kg is found for MnAs/GaAs(001). Our results reveal that it is possible to handle MCE and refrigerating power by using the epitaxial constraints without a detrimental reduction in the magnetostructural transition temperature.

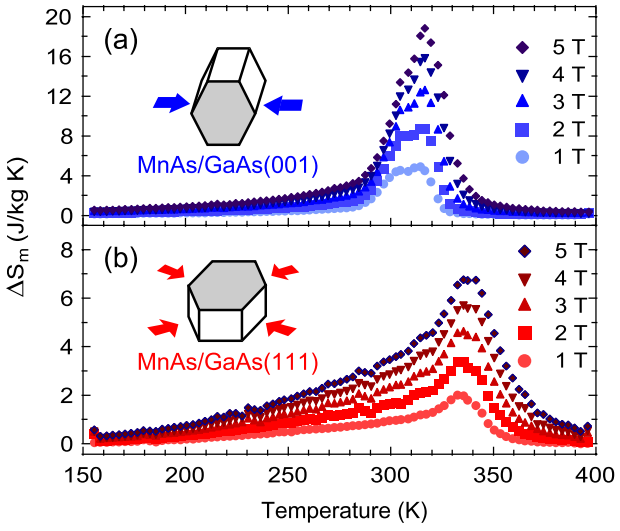

FIG. 3 (color online). Magnetic-entropy changes as a function of temperature and field for (a) MnAs/GaAs(001) and (b) MnAs/GaAs(111) epilayers. The magnetic field was applied parallel to the easy magnetic axis of the MnAs epilayers.

The impact of strain on the α-β transition can be modeled using a simple thermodynamical approach by considering an hypothetical homogeneously strained MnAs system (the issue of phase coexistence is not considered here). A simplified form of the free energy is given by

$$F = -\frac{3}{2}\frac{J}{J+1} N k_B T_C \sigma^2 - H g \mu_B J N \sigma + E_{\mathrm{el}} - T S_m, \tag{1}$$

where the terms are the exchange energy under the molecular field approximation, the Zeeman energy, the elastic energy (E_{el}) and the term related to magnetic entropy S_m. T_C is the Curie temperature, J is the angular momentum, N is the density of magnetic ions, k_B is the Boltzmann constant, μ_B is the Bohr magneton, $\sigma = M/M_S$ is the normalized magnetization, g is the Landé factor, and H the external magnetic field. For an in-plane biaxial strain, in the case of MnAs/GaAs(111), $E_{\mathrm{el}} = \frac{Y}{1-\nu}(\epsilon - \eta)^2$, where Y is the Young modulus, ν the Poisson ratio, ϵ the in-plane strain and η the thermal strain. The magneto-structural coupling arises from the dependence of T_C on the strain components

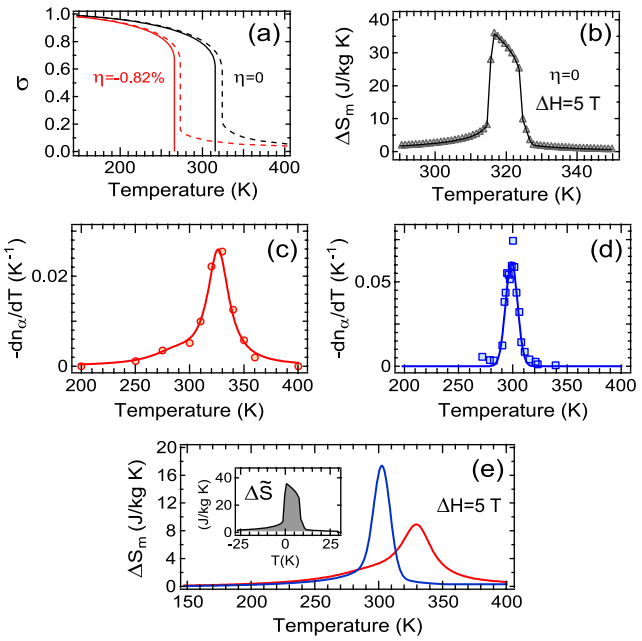

FIG. 4 (color online). (a) Calculated reduced magnetization for strained MnAs epilayers. (b) Calculated magnetocaloric effect for unstrained MnAs. (c)–(d) Absolute values of the derivatives of the α-phase fraction as a function of the temperature for MnAs/Gas(111) and MnAs/GaAs(001). The values for MnAs/GaAs(001) were deduced from optical spectroscopy measurements (cf. Ref. [19]) and the values for MnAs/GaAs(111) from neutron diffraction measurements (cf. Ref. [14]). The dotted lines are fitted curves. (e) Modeled MCE curves obtained by convoluting the fitted curves of $-\partial n_\alpha/\partial T$ and $\Delta \tilde{S}$ (inset).

$$T_C = T_0(1 + \kappa_a \epsilon_a + \kappa_b \epsilon_b + \kappa_c \epsilon_c). \quad (2)$$

DFT calculation by Runger and Sanvito showed that κ_a, $\kappa_b > 5|\kappa_c|$; i.e., an extension in the basal plane leads to T_C enhancement and the magnetic order is much less sensitive to deformation along the c axis. These trends are confirmed by experimental results obtained on MnAs/GaAs(001) and MnAs/GaAs(111). We therefore use the following simplified expression of Eq. (2):

$$T_C = T_0(1 + 2\kappa\epsilon), \quad (3)$$

where ϵ is the mean strain in the basal plane and κ is an adjustable parameter. Similarly to Ref. [2], we are thus dealing with a modified Bean-Rodbell model. From the minimization of F, one extracts $\sigma(T)$ and ΔS_m for given values of η. Taking $T_0 = 290$ K, $J = 1.72$, $\kappa = 13$, it is possible to reproduce reasonably well $\sigma(T)$ of an unstrained MnAs sample [Fig. 4(a)]. A compressive strain of 0.82%, as measured in MnAs/GaAs(111) [14], leads to a transition at 266 K [Fig. 4(a)] in fair agreement with the temperature of premature β appearance. The magnetization under applied magnetic field can also be calculated and the magnetic-entropy variation, ΔS_m [plotted in Fig. 4(b) for $\Delta H = 5$ T], can de deduced from values of σ with and without magnetic field within the mean-field approximation [9,11].

Considering previous statements on the magnetostructural behavior of strained MnAs epilayers, the picture that emerges concerning the magnetocaloric effect is the following: as the α-β phase transition remains first-order in the coexistence region, the entropy variation at a given temperature T is proportional to the fraction of MnAs transforming from α to β between T and $T + \delta T$ ($\delta T \ll T$), $\delta n_{\alpha\to\beta} = -(\partial n_\alpha/\partial T)\delta T$ and to $\Delta\tilde{S}_\eta(T)$, the entropy variation for a hypothetical α-MnAs epilayer with homogeneous strain η in the basal plane at temperature T. As a first approximation, we shall consider that the $\Delta\tilde{S}_\eta(T)$ profile is constant throughout the phase coexistence region, then

$$\Delta S(T) \simeq -\int_0^{+\infty} \Delta\tilde{S}(T-u)\left(\frac{\partial n_\alpha}{\partial u}\right)du. \quad (4)$$

From values of n_α obtained by neutron diffraction and optical spectroscopy on both MnAs/GaAs(111) [14] and MnAs/GaAs(001) [19], the thermal evolutions of $-\partial n_\alpha/\partial T$ were obtained and plotted in Fig. 4(c) and 4(d). These curves were fitted and the fitted profiles were convoluted with the $\Delta\tilde{S}$ function extracted from the mean-field calculation. The results are displayed in Fig. 4(e) for $\Delta H = 5$ T. A close similarity with the $\Delta S(T)$ profiles displayed in Fig. 3 can be seen. The agreement is quite good, the difference in magnitude between the experimental and simulated profiles for MnAs/GaAs(111) may be due to poor statistics concerning the $\partial n_\alpha/\partial T$ data. This close agreement justifies our assumptions *a posteriori* and show that the MCE intensity in MnAs does not depend sensitively on strain and can be explained solely on the basis of a magnetic-entropy variation. It is not necessary to invoke large electronic and/or lattice contributions in order to explain the amplitude of the MCE in MnAs epilayers, in agreement with recent measurements reported by Zou *et al.* [9]. The MCE, although not entering the so-called *colossal* regime, remains *giant* and its spread and maximal position are tuned through the epitaxy dependent thermal strain η that controls n_α.

To conclude, it is not clear if bulk MnAs will really get to the stage of real-life applications in commercially competitive magnetic refrigerator. However, the compatibility of MnAs ferromagnetic α phase with Si(001), GaAs(001) and GaAs(111) semiconductor substrates [20–26] suggests a further interesting route for MnAs-based magnetocaloric applications. In this respect, the integration of the magnetic refrigeration process with microelectronic circuitry using the stray magnetic fields as well as spintronics devices (e.g., thermally assisted magnetoresistive random-access memories) are possible and attractive perspectives foreseen.

The authors acknowledge financial support from CAPES-COFECUB Program, CNPq, ANR PNANO Program and C'nano Île-de-France. D. Demaille and Y. Zheng are greatly acknowledged for providing support in transmission microscopy and magnetic measurements.

[1] K. A. Gschneidner, Jr., V. K. Pecharsky, and A. O. Tsokol, Rep. Prog. Phys. **68**, 1479 (2005).
[2] P. J. von Ranke *et al.*, Phys. Rev. B **73**, 014415 (2006).
[3] O. Tegusa *et al.*, Physica (Amsterdam) **319B**, 174 (2002).
[4] S. Gama *et al.*, Phys. Rev. Lett. **93**, 237202 (2004).
[5] A. de Campos *et al.*, Nature Mater. **5**, 802 (2006).
[6] D. L. Rocco *et al.*, Appl. Phys. Lett. **90**, 242507 (2007).
[7] H. Wada and Y. Tanabe, Appl. Phys. Lett. **79**, 3302 (2001).
[8] G. J. Liu *et al.*, Appl. Phys. Lett. **90**, 032507 (2007).
[9] J. D. Zou *et al.*, Europhys. Lett. **81**, 47002 (2008).
[10] B. T. M. Willis and H. P. Rooksby, Proc. Phys. Soc. London Sect. B **67**, 290 (1954).
[11] C. P. Bean and D. S. Rodbell, Phys. Rev. **126**, 104 (1962).
[12] R. H. Wilson and J. S. Kasper, Acta Crystallogr. **17**, 95 (1964).
[13] J. Mira *et al.*, Phys. Rev. Lett. **90**, 097203 (2003).
[14] V. Garcia *et al.*, Phys. Rev. Lett. **99**, 117205 (2007).
[15] I. Rungger and S. Sanvito, Phys. Rev. B **74**, 024429 (2006).
[16] F. Iikawa *et al.*, Phys. Rev. Lett. **95**, 077203 (2005).
[17] C. Adriano *et al.*, Appl. Phys. Lett. **88**, 151906 (2006).
[18] H. Yamaguchi *et al.*, Europhys. Lett. **72**, 479 (2005).
[19] F. Vidal *et al.*, Phys. Rev. B **74**, 115330 (2006).
[20] M. Tanaka *et al.*, J. Vac. Sci. Technol. B **12**, 1091 (1994).
[21] M. Tanaka *et al.*, J. Appl. Phys. **76**, 6278 (1994).
[22] M. Tanaka, Physica (Amsterdam) **2E**, 372 (1998).
[23] V. M. Kaganer *et al.*, Phys. Rev. Lett. **85**, 341 (2000).
[24] F. Schippan *et al.*, J. Appl. Phys. **88**, 2766 (2000).
[25] L. Däweritz, Rep. Prog. Phys. **69**, 2581 (2006).
[26] J. Varalda *et al.*, J. Appl. Phys. **100**, 093524 (2006).